

RESEARCH ARTICLE | JUNE 15 2020

Cantilever-based ferroelectret energy harvesting

O. Ben Dali   ; P. Pondrom  ; G. M. Sessler  ; S. Zhukov  ; H. von Seggern  ; X. Zhang  ;
M. Kupnik 

 Check for updates

Appl. Phys. Lett. 116, 243901 (2020)

<https://doi.org/10.1063/5.0006620>



APL Energy

Latest Articles Online!

Read Now



Cantilever-based ferroelectret energy harvesting

Cite as: Appl. Phys. Lett. **116**, 243901 (2020); doi: 10.1063/5.0006620

Submitted: 4 March 2020 · Accepted: 29 May 2020 ·

Published Online: 15 June 2020



View Online



Export Citation



CrossMark

O. Ben Dali,^{1,a)} P. Pondrom,¹ G. M. Sessler,² S. Zhukov,³ H. von Seggern,³ X. Zhang,⁴ and M. Kupnik¹

AFFILIATIONS

¹Measurement and Sensor Technology, Technische Universität Darmstadt, Merckstraße 25, 64283 Darmstadt, Germany

²Institute für Telecommunications Technology, Technische Universität Darmstadt, Merckstraße 25, 64283 Darmstadt, Germany

³Electronic Materials, Technische Universität Darmstadt, Merckstraße 25, 64283 Darmstadt, Germany

⁴School of Physics Science and Engineering, Tongji University, Siping Road 1239, Shanghai 200092, China

^{a)} Author to whom correspondence should be addressed: dali@must.tu-darmstadt.de

ABSTRACT

We present a vibrational energy harvester with fluorinated ethylene propylene (FEP)-ferroelectrets working in d_{31} mode. The ferroelectret film consists of two FEP films, fused together to form a parallel tunnel structure with well-defined air gaps. Its dynamic piezoelectric g_{31} coefficient is 0.7 V m N^{-1} . The energy-harvesting device is an air-spaced cantilever arrangement that was produced by the additive manufacturing technique. The device was tested by exposing it to sinusoidal vibrations with an acceleration a , generated by a shaker. The measurement shows a resonance at about 35 Hz and a normalized output power of $320 \mu\text{W}$ for a seismic mass of 4.5 g at an acceleration of 0.1 g (g is the gravity of the earth). This demonstrates a significant improvement of air-spaced vibrational energy harvesting with ferroelectrets and greatly exceeds previous performance data for polymer cantilever devices.

Published under license by AIP Publishing. <https://doi.org/10.1063/5.0006620>

For many applications, such as structural health monitoring, medical applications, autonomous vehicles, and environmental monitoring systems, the need for sensor networks steadily increases. Often, the sensors are positioned at remote places where the availability of electrical power or possibilities, such as replacing or recharging batteries, are challenging tasks. Therefore, other methods for powering electronic circuitry, such as energy harvesting, have been a growing field of study for the last 20 years.¹⁻⁵ Energy harvesting may be defined as the conversion of energy from environmental (thermal, optical, and mechanical) sources into electrical energy. Vibration-based energy harvesters, as studied here, belong to the category of mechanical conversion devices. They are typically mass-spring systems with intentionally low resonance frequencies. Since environmental mechanical vibrations usually have the highest amplitude around or below 100 Hz, setting the resonance frequency of the device to such values allows us to maximize the generation of electrical energy. The four main transduction methods for energy conversion used for vibration-based energy harvesting are electrostatic, electromagnetic, piezoelectric, and triboelectric.

The efficiency of piezoelectric energy harvesters depends mainly on the sensitivity of the used piezoelectric materials. In order to improve the performance of these energy harvester systems, more sensitive piezoelectric materials have been investigated.⁶ The dominating materials for energy harvesting application have been inorganic

piezoelectric materials due to their remarkable performance and mechanical stability. Some of these high-performance piezoelectric materials, such as lead zirconate titanate (PZT), contain lead, which is considered as a toxic substance. In comparison to inorganic piezoelectric materials, piezoelectric polymers show more flexibility and are easy to process. However, they exhibit smaller piezoelectric activity. A promising development of such piezoelectric polymers, namely, the ferroelectrets, overcomes this drawback, which have shown high piezoelectric coefficients similar to those of commercial PZT films.

Ferroelectrets (also called piezoelectrets)⁷⁻⁹ have been investigated for 20 years. Early ferroelectrets were cellular polymers exhibiting a high piezoelectric activity after electrical poling and surface metallization. For a long time, the main ferroelectret material has been cellular polypropylene (PP) that possesses large longitudinal piezoelectric d_{33} and g_{33} coefficients but exhibits almost no transverse piezoelectric activity. In addition, PP has a limited thermal piezoelectric d_{33} stability.^{10,11} First, ferroelectret energy harvesters were introduced in 2012.^{12,13} The possibility of folding and stacking such films allows us to increase the generated power and decrease the resonance frequency of energy harvesters without increasing the seismic mass. This results in compact and lightweight energy harvesters with relatively high power output.^{14,15} Due to the high viscosity of cellular polypropylene, the width of the resonance peak of such energy harvesters is generally larger than that of conventional ceramic piezoelectric devices.

Due to the aforementioned limited thermal stability and the minute transverse piezoelectric activity of cellular polypropylene, alternative ferroelectret materials have been investigated.^{16–25} In particular, parallel-tunnel or tubular-channel fluorinated ethylene propylene (FEP) ferroelectret films were used. Such samples, described before,^{23,24} are manufactured utilizing a 12.5 μm thick FEP film. The piezoelectrically relevant air tunnels of the ferroelectret film, however, have a thickness of several hundred micrometers [see Fig. 1(a)]. These samples exhibit strong transverse as well as longitudinal piezoelectric coefficients.^{23,24} The working mechanism is shown schematically in previous work.²⁴ Because of the superior electret properties of FEP, its temperature stability is far better than that of polypropylene.^{18,26–28} Using the high piezoelectric transverse coefficient of parallel-tunnel FEP ferroelectrets, it was possible to realize energy harvesters where the seismic mass lies in the middle of such a strip and dynamically stretches it in response to input acceleration, generating high output powers at resonance frequencies around 60 Hz with a small seismic mass as low as 0.1 g.^{23,24} However, such harvesters are not considered to be robust and their performance depends on their orientation with respect to gravity. Therefore, more rugged alternative solutions using the parallel-tunnel FEP ferroelectrets will be investigated in this paper. The ferroelectret energy harvester basically consists of a cantilever made by the additive manufacturing technique (3D-printing) utilizing the extrusion of polylactide acid (PLA). On top at a certain distance h , there is a parallel-tunnel FEP ferroelectret film whose working mechanism is shown in previous work.²⁴ It is dynamically stretched by the cantilever beam via a seismic mass structure, when the cantilever base is subjected to an acceleration a (see Fig. 1). The orientation of the tunnels is perpendicular to the cantilever direction.

When the support, and, thus, the cantilever, is subjected to an acceleration a , the seismic mass is deflected in the z -direction from its position of equilibrium and forms an angle φ with the cantilever's plane [Fig. 1(b)]. For small deflections, the displacement of the cantilever tip in the x -direction has been neglected. The angle φ can then be expressed as^{29,30}

$$\varphi = \frac{3}{2} \frac{z}{L_C}, \quad (1)$$

where L_C is the length of the cantilever. The variation of the length of the ferroelectret film in the x -direction is then geometrically determined as

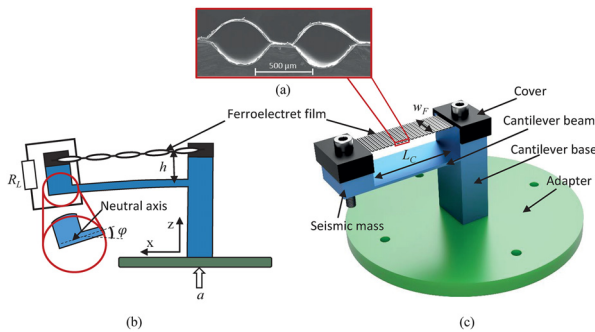


FIG. 1. (a) Cross section of a parallel-tunnel FEP ferroelectret film. (b) Schematic representation of the cantilever structure in the bending condition. (c) 3D representation of the air-spaced cantilever energy harvester.

$$\Delta l = h\varphi = \frac{3hz}{2L_C}. \quad (2)$$

Hence, only for small deflections, the stretching of the film is proportional to its distance h from the neutral axis of the cantilever beam.^{31–33}

Then, the power generated by the ferroelectret film, with capacitance C and piezoelectric voltage constant g_{31} in a load resistance R_L , can be expressed similar to that of a ferroelectret nanogenerator based on the g_{31} effect, while taking the correct geometric variation of the length into account,²⁴ i.e.,

$$P_R = \left(g_{31} \frac{3h k_F}{2L_C w_F} \right)^2 \times \frac{a^2 R_L C^2 \omega^2 / \omega_0^4}{\left(1 - \left(\frac{\omega}{\omega_0} \right)^2 \right)^2 + 4 \xi^2 \left(\frac{\omega}{\omega_0} \right)^2} (1 + (R_L C \omega)^2), \quad (3)$$

where ω is the circular frequency of acceleration a , ω_0 the resonance frequency of the beam including the seismic mass, k_F and w_F the film's tensile stiffness and width, respectively, and ξ cantilever's damping ratio. The maximal power at the resonance frequency, for the optimal load resistance $R_{opt} = 1/C\omega_0$, amounts to

$$P_R = \left(g_{31} \frac{3h k_F}{2L_C w_F} \right)^2 \frac{C}{8\xi^2 \omega_0^3} a^2 = \frac{9}{32} \frac{h^2}{L_C^2 \xi^2 \omega_0^3} \frac{k_F^2}{w_F^2} g_{31}^2 C a^2. \quad (4)$$

Equation (4) shows that P_{opt} of a cantilever-based ferroelectret energy harvester exhibits the same dependence on the resonance frequency as a ferroelectret energy harvester based on the d_{33} effect.¹⁴ Apart from the properties of the cantilever beam and from the ferroelectret film, the parameter with the major influence on the generated power is the distance h between the film and the neutral axis of the beam. The authors are well aware of the fact that increasing h leads to a nonlinear stretching of the film. For larger h or large acceleration a , the growth of ΔL is restrained due to increasing restoring force of the ferroelectret film described by k_F . This leads to an increase in the stiffness of the film-cantilever system and an increase in the resonance frequency. For the presented cantilever geometry, the measurement of the resonance frequency of the cantilever structure with and without the ferroelectret film shows a difference of approximately 2 Hz (see Fig. 2).

In the following, an experimental validation of the above analytical model is demonstrated. In the experimental setup, a cantilever-based ferroelectret harvester such as presented above in Fig. 1(c) is placed on an electrodynamic shaker (Brüel and Kjær 4809). The signal is delivered to the shaker using a function generator (Keysight 33500B Series) and a power amplifier (B&K 2718). The charge generated by the harvester is measured using a charge amplifier (B&K Nexus) and a digital oscilloscope (Rohde and Schwartz RTB 2004). The parameters used for the calculations of the generated power via Eq. (3) are summarized in Table I.

The film capacitance was measured using an impedance meter (LCR Databridge 451). The g_{31} coefficient and ferroelectret film stiffness k_F were taken from the literature.²⁴ In addition, the film utilized has the same length and width as previously used,^{23,24} in order to be able to compare the generated power (Table II). The fit of

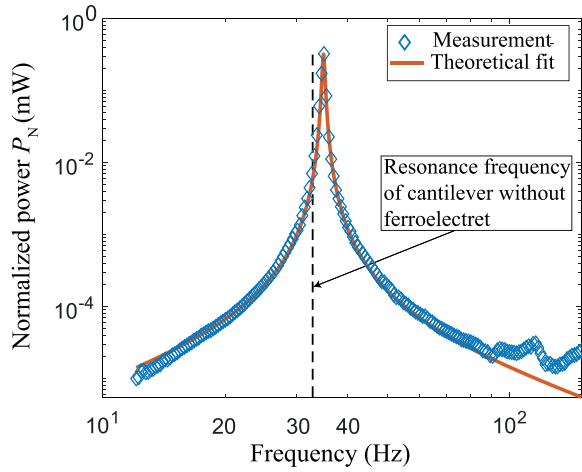


FIG. 2. Normalized power of a cantilever-based ferroelectret energy harvester with a distance h of 1 cm between the ferroelectret film and the cantilever neutral axis and a seismic mass of 4.5 g. The theoretical curve was calculated from Eq. (3) using parameters of Table I. The actual acceleration at the resonance frequency amounts to 0.1 g, whereas the normalized power was calculated using Eq. (6). Also shown (dashed line) is the resonance frequency of the cantilever without the ferroelectret.

experimental results to Eq. (3) was used to determine the variables ξ , while other parameters listed in Table I were treated as experimentally verified for the fitting procedure. Two methods are possible for the measurement of the generated power: either a resistance of the optimal value R_{opt} is connected between the two electrodes of the ferroelectret film and the power generated in R_{opt} is calculated from the measured charge, or the power is estimated from the charge generated in the short circuit using the following equation:¹⁴

$$P_R = (q_{sc,rms}\omega)^2 \frac{R_{opt}}{(1 + (R_{opt} C \omega)^2)}. \quad (5)$$

The normalized power P_N is defined as the power generated by the energy harvester extrapolated to an acceleration of $g = 9.81 \text{ ms}^{-2}$, which is the gravitational acceleration, i.e.,

$$P_N = \left(\frac{g}{a}\right)^2 P_R. \quad (6)$$

TABLE I. Parameters for the calculations of Fig. 2.

Parameters	Fit values	Source
g_{31} (V m/N)	0.7	Reference 23
C (pF)	40	Measurement
h (mm)	10	Measurement
L_C (mm)	30	Measurement
w_F (mm)	10	Measurement
R_l (M Ω)	113	Measurement
k_F (N/m)	500	Calculated from Ref. 23
f_0 (Hz)	34.7	Measurement
ξ	0.0084 ± 0.0001	Fit

TABLE II. Normalized power generated by various kinds of ferroelectret energy harvesters including the one presented in the present paper. Normalizing the power takes into account that the generated power is proportional to a^2 .

Type of harvester	Normalized power (μW)	Resonance frequency (Hz)	Size of active area (cm^2)
Ferroelectret g_{33} IXPP ($m_s = 33.7 \text{ g}$) ³⁴	120	800	3.14
Ferroelectret g_{31} ($m_s = 2 \text{ g}$) ²³	230	30	3
Ferroelectret g_{31} advanced design ($m_s = 0.3 \text{ g}$) ²⁴	109	58	0.4
Ferroelectret cantilever g_{31} ($m_s = 4.5 \text{ g}$) (Fig. 1)	320	35	3

The measurement of the normalized power P_N , generated by a ferroelectret energy harvester into a load resistance R_l (Fig. 2), agrees well with the fit result obtained from Eq. (3). At frequencies well below resonance, P_N increases proportional to ω^2 , and at frequencies above resonance, it decreases proportional to $1/\omega^4$. Referred to the seismic mass of 4.5 g and to the applied acceleration of 0.1 g, a maximum normalized power of 320 μW at resonance is achieved.

The dependence of the generated power on acceleration applied to the cantilever was studied as well. The cantilever was subjected to various acceleration amplitudes ranging from 0.005 g to 0.5 g (RMS). A seismic mass of 4.5 g (tip mass) was used in all cases. The generated power at resonance was measured for each acceleration amplitude [Fig. 3(a)].

Below an acceleration of 0.06 g, the generated power is proportional to a^2 , as expected from Eqs. (4) and (5). Referred to an RMS value of 1 g, the results correspond to a normalized power of approximately 0.8 mW [Fig. 3(b)]. For $a > 0.06 \text{ g}$, the generated power increases less than proportional to a^2 , reaching a normalized value of $P_N = 80 \mu\text{W}$ for $a = 0.5 \text{ g}$. This decrease can be explained by the mechanical behavior of the ferroelectret film in the two stages of deformation developed during upward and downward cycles. When the cantilever is bent upward [Fig. 3(c)] for large amplitude vibrations, the film as such is bent instead of being compressed and the power, thus, starts to saturate, as evident from Fig. 3(d). On the other hand, when the cantilever is bent downwards, the film is excessively stretched for large amplitude vibrations. In such a case, the stiffness of the ferroelectret film increases and results in a smaller deformation or equivalently to a smaller g_{31} coefficient. In addition, the damping of the FEP layers becomes more severe. A detailed investigation of these effects is beyond the scope of this paper and will be published separately.

Finally, the influence of the seismic mass on the frequency response and maximum generated power at resonance was investigated. Various masses were added to the tip of the cantilever, and the corresponding frequency responses were measured. The tip mass without an additional mass amounts to 4 g, whereas the maximum mass equals 12.1 g. The resonance frequency of the energy harvester decreases proportional to $1/\sqrt{m_s}$, and the normalized power at resonance frequency is proportional to $m_s^{3/2}$ (Fig. 4). This relation between P_N and m_s follows from Eq. (3) using the relation $\omega_0^2 = k_C/m_s$, where k_C is the spring constant of the complete energy harvester.

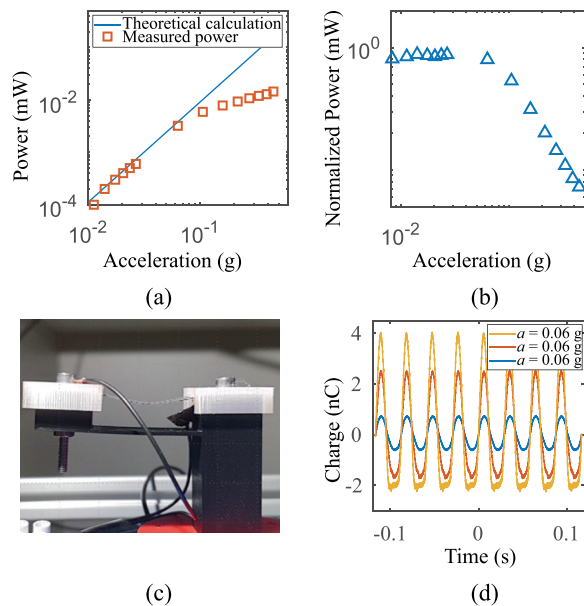


FIG. 3. (a) Power generated by a cantilever-based ferroelectret energy harvester at resonance as a function of the input acceleration for a seismic mass of 4.5 g. (b) Normalized power as a function of input acceleration. (c) Temporal waveform of the generated power for various input accelerations. (d) Photograph of a cantilever-based ferroelectret energy harvester at resonance for $a = 0.43$ g.

In conclusion, energy harvesting with ferroelectrets in conjunction with a cantilever arrangement has been realized and discussed. In the setup used, the ferroelectret and the cantilever are separated by a large air gap. This leads to a significantly increased extension of the ferroelectret upon bending of the cantilever at least for one bending direction. For a seismic mass of 4.5 g, such a harvester generates a normalized output power of $320 \mu\text{W}$ at its resonance frequency of about 35 Hz and for an acceleration of 0.1 g. This is in excellent agreement with theory, as well as the dependence of the resonance frequency and the generated power on the seismic mass. For accelerations above 0.05 g, however, the normalized power outputs do not exceed 1 mW with the present harvester. It is expected that the range of power can be extended for higher accelerations with a modified harvester design using mechanical pre-stressing.

The robustness of the cantilever-based ferroelectret energy harvesters discussed in this paper is significantly better than that of previously described ferroelectret nanogenerators.²⁴ In addition, the preliminary results show a stable performance up to 10^7 cycles at room temperature (not graphically shown).

As shown in Table II, the normalized power exceeds that of previously described ferroelectret nanogenerators and is far above that of the conventional piezoelectret energy harvesters based on the longitudinal piezoeffect. Its more robust design is, however, a great advantage and should help the present harvester to become acceptable for application in spite of its relatively large seismic mass. Depending on the specific requirements for a given application, such as robustness, high normalized power, small mass, miniature size, or suitable resonance frequency, one finds in the table a useful selection of appropriate energy harvesting techniques to choose from.

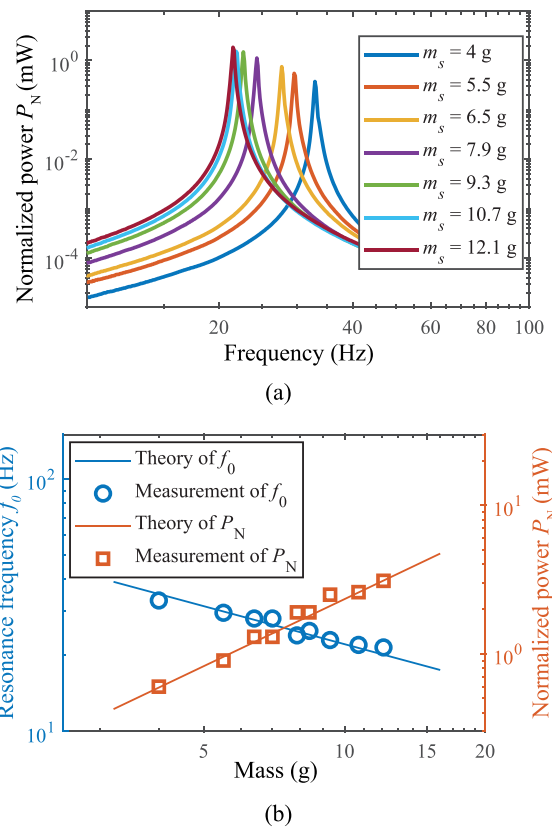


FIG. 4. (a) Measured frequency responses of the normalized power of an energy harvester with various seismic masses including the tip mass. (b) Normalized power at resonance and resonance frequency as a function of seismic mass. The theoretical curves are fitted, using the expected slopes.

This work was supported by Deutsche Forschungsgemeinschaft (DFG) Grant Nos. KU 3498/1-1, SE 941/19-1, and SE 941/21-1, and National Natural Science Foundation of China (NSFC) Grant No. 61761136004.

DATA AVAILABILITY

The data that support the findings of this study are available from the corresponding author upon reasonable request.

REFERENCES

- S. R. Anton and H. A. Sodano, "A review of power harvesting using piezoelectric materials (2003–2006)," *Smart Mater. Struct.* **16**, R1–R21 (2007).
- A. Erturk and D. J. Inman, *Piezoelectric Energy Harvesting* (Wiley, Chichester, West Sussex, UK/Hoboken, NJ, 2011).
- Micro Energy Harvesting*, Advanced Micro and Nanosystems, edited by D. Briand, E. Yeatman, and S. Roundy (Wiley-VCH Verlag GmbH & Co. KGaA, Weinheim, 2015).
- S. Priya and D. J. Inman, *Energy Harvesting Technologies* (Springer, New York, 2009).
- T. J. Kaźmierski and S. Beeby, *Energy Harvesting Systems: Principles, Modeling and Applications* (Springer Science + Business Media LLC, New York, NY, 2011).

- ⁶H. Liu, J. Zhong, C. Lee, S.-W. Lee, and L. Lin, "A comprehensive review on piezoelectric energy harvesting technology: Materials, mechanisms, and applications," *Appl. Phys. Rev.* **5**, 041306 (2018).
- ⁷R. M. Faria, "A direct current piezoelectric effect in fluorinated ethylene-propylene copolymer due to space charge," *Appl. Phys. Lett.* **69**, 1972–1974 (1996).
- ⁸G. M. Sessler and J. Hillenbrand, "Electromechanical response of cellular electret films," *Appl. Phys. Lett.* **75**, 3405–3407 (1999).
- ⁹S. Bauer, R. Gerhard-Multhaupt, and G. M. Sessler, "Ferroelectrets: Soft electroactive foams for transducers," *Phys. Today* **57**(2), 37–43 (2004).
- ¹⁰X. Zhang, J. Hillenbrand, and G. M. Sessler, "Improvement of piezoelectric activity of cellular polymers using a double-expansion process," *J. Phys. D* **37**, 2146–2150 (2004).
- ¹¹A. Mellinger, M. Wegener, W. Wirges, R. R. Mallepally, and R. Gerhard-Multhaupt, "Thermal and temporal stability of ferroelectret films made from cellular polypropylene/air composites," *Ferroelectrics* **331**, 189–199 (2006).
- ¹²S. R. Anton and K. M. Farinholt, "An evaluation on low-level vibration energy harvesting using piezoelectret foam," *Proc. SPIE* **8341**, 83410G (2012).
- ¹³S. R. Anton, K. M. Farinholt, and A. Erturk, "Piezoelectret foam-based vibration energy harvesting," *J. Intell. Mater. Syst. Struct.* **25**, 1681–1692 (2014).
- ¹⁴P. Pondrom, J. Hillenbrand, G. M. Sessler, J. Bö, and T. Melz, "Vibration-based energy harvesting with stacked piezoelectrets," *Appl. Phys. Lett.* **104**, 172901 (2014).
- ¹⁵G. M. Sessler, P. Pondrom, and X. Zhang, "Stacked and folded piezoelectrets for vibration-based energy harvesting," *Phase Transitions* **89**, 667–677 (2016).
- ¹⁶S. Zhukov, H. von Seggern, X. Zhang, Y. Xue, O. Ben Dali, P. Pondrom, G. M. Sessler, and M. Kupnik, "Microenergy harvesters based on fluorinated ethylene propylene piezotubes," *Adv. Eng. Mater.* **22**, 1901399 (2020).
- ¹⁷R. A. P. Altafim, X. Qiu, W. Wirges, R. Gerhard, R. A. C. Altafim, H. C. Basso, W. Jenninger, and J. Wagner, "Template-based fluoroethylenepropylene piezoelectrets with tubular channels for transducer applications," *J. Appl. Phys.* **106**, 014106 (2009).
- ¹⁸X. Zhang, J. Hillenbrand, G. M. Sessler, S. Haberzettl, and K. Lou, "Fluoroethylenepropylene ferroelectrets with patterned microstructure and high, thermally stable piezoelectricity," *Appl. Phys. A* **107**, 621–629 (2012).
- ¹⁹H. von Seggern, S. Zhukov, and S. Fedosov, "Importance of geometry and breakdown field on the piezoelectric d_{33} coefficient of corona charged ferroelectret sandwiches," *IEEE Trans. Dielectr. Electr. Insul.* **18**, 49–56 (2011).
- ²⁰B.-X. Xu, H. von Seggern, S. Zhukov, and D. Gross, "Continuum modeling of charging process and piezoelectricity of ferroelectrets," *J. Appl. Phys.* **114**, 094103 (2013).
- ²¹S. Zhukov, D. Eder-Goy, C. Biethan, S. Fedosov, B.-X. Xu, and H. von Seggern, "Tubular fluoropolymer arrays with high piezoelectric response," *Smart Mater. Struct.* **27**, 015010 (2018).
- ²²S. Zhukov, D. Eder-Goy, S. Fedosov, B.-X. Xu, and H. von Seggern, "Analytical prediction of the piezoelectric d_{33} response of fluoropolymer arrays with tubular air channels," *Sci. Rep.* **8**, 4597 (2018).
- ²³X. Zhang, P. Pondrom, L. Wu, and G. M. Sessler, "Vibration-based energy harvesting with piezoelectrets having high d_{31} activity," *Appl. Phys. Lett.* **108**, 193903 (2016).
- ²⁴X. Zhang, P. Pondrom, G. M. Sessler, and X. Ma, "Ferroelectret nanogenerator with large transverse piezoelectric activity," *Nano Energy* **50**, 52–61 (2018).
- ²⁵O. Ben Dali, S. Zhukov, R. Chadda, P. Pondrom, X. Zhang, G. Sessler, H. von Seggern, and M. Kupnik, "Modeling of piezoelectric coupling coefficients of soft ferroelectrets for energy harvesting," in *2019 IEEE International Ultrasonics Symposium (IUS)* (IEEE, 2019), pp. 2454–2457.
- ²⁶X. Zhang, J. Hillenbrand, and G. M. Sessler, "Thermally stable fluorocarbon ferroelectrets with high piezoelectric coefficient," *Appl. Phys. A* **84**, 139–142 (2006).
- ²⁷H. von Seggern, S. Zhukov, and S. Fedosov, "Poling dynamics and thermal stability of FEP/ePTFE/FEP sandwiches," *IEEE Trans. Dielectr. Electr. Insul.* **17**, 1056–1065 (2010).
- ²⁸R. P. Altafim, D. Rychkov, W. Wirges, R. Gerhard, H. Basso, R. Correa Altafim, and M. Melzer, "Laminated tubular-channel ferroelectret systems from low-density polyethylene films and from fluoroethylene-propylene copolymer films: A comparison," *IEEE Trans. Dielectr. Electr. Insul.* **19**, 1116–1123 (2012).
- ²⁹K.-H. Grote, *Dubbel: Taschenbuch für den Maschinenbau*, 22nd ed. (Springer-Verlag, 2007).
- ³⁰T. Beléndez, C. Neipp, and A. Beléndez, "Large and small deflections of a cantilever beam," *Eur. J. Phys.* **23**, 371–379 (2002).
- ³¹A. Kachroudi, S. Basrour, L. Rufer, and F. Jomni, "Air-spaced PDMS piezoelectret cantilevers for vibration energy harvesting," *J. Phys.* **773**, 012072 (2016).
- ³²S. Boisseau, G. Despesse, and A. Sylvestre, "Optimization of an electret-based energy harvester," *Smart Mater. Struct.* **19**, 075015 (2010).
- ³³S. Boisseau, G. Despesse, T. Ricart, E. Defay, and A. Sylvestre, "Cantilever-based electret energy harvesters," *J. Appl. Phys.* **20**, 105013 (2011).
- ³⁴X. Zhang, L. Wu, and G. M. Sessler, "Energy harvesting from vibration with cross-linked polypropylene piezoelectrets," *AIP Adv.* **5**, 077185 (2015).